Korea-Australia Rheology Journal
Vol. 17, No. 3, September 2005 pp. 111-116

Modelling nonlinear polymer rheology is still challenging

Giuseppe Marrucci* and Giovanni Ianniruberto
Università Federico II, Piazzale Tecchio 80, I-80125 Napoli, Italy
(Received April 19, 2005)

Abstract

The new tube model with variable diameter (Marrucci and Ianniruberto, 2004), recently introduced to interpret new elongational data of polymer melts, is here extended to encompass arbitrary flows, specifically shear flows. The predicted results compare well with existing data of entangled polymer melts. Challenges still remain when the comparison is extended to recent elongational data on entangled solutions by Sridhar.

1. Introduction

It is well known that the rheological response of polymer melts and concentrated solutions is dominated by the entanglement phenomenon, and much progress has been made in modelling these systems in both the linear and nonlinear viscoelastic range. However, while modelling in the linear range seems to have reached a very good level of description, the nonlinear behaviour in fast flows is still open to possible improvement. In particular, the most popular tube models do not seem compatible with recent accurate data of elongational viscosity on polystyrene melts by Hassager *et al.* (2003) and on polystyrene solutions by Sridhar *et al.* (2005).

We have recently shown that Hassager's data can be interpreted in terms of a modified tube model, where the tube diameter decreases with increasing the stretching rate of the elongational flow. The idea that tubes may change their diameter during flow is not new, and has been particularly defended by Wagner *et al.* (1992; 2001). However, the way the problem is dealt with in our recent work (Marrucci and Ianniruberto, 2004) is in fact original.

The result previously obtained was limited to steady elongational flows, and a comparison was successfully made with Hassager's data. Nonlinear rheology must nevertheless encompass other flows, particularly shear as well as elongation, and transient flows as well as steady. In this paper therefore, the model previously advanced is extended to arbitrary flow conditions, and a general appraisal of its predictions is made.

2. The model

The main novelties introduced in our previous paper (Marrucci and Ianniruberto, 2004) are: i) the pressure effect due to interchain repulsive interactions, ii) the resulting dynamics of tube diameter under flow, and iii) the characteristic time of tube diameter relaxation. Before presenting the complete model, these items are briefly reviewed.

We assume, as often done in the past, that the tube tends to deform affinely. As a consequence of that assumption, the elongational flow would squeeze tubes, reducing their diameter. However interchain interactions oppose such a tendency, and we represent the repulsive interaction through a thermal pressure p on tube wall. Classical kinetic theory then gives (Marrucci and Ianniruberto, 2004; Doi and Edwards, 1986)

$$p \approx kT\frac{Nb^2}{a^4 L} \tag{1}$$

where kT is thermal energy, N and b are number and length of Kuhn segments (or "monomers"), respectively, and a and L are diameter and length of the tube segment containing those monomers. The near-equality sign in Eq. (1) means that the numerical coefficient of order unity is ignored. From the pressure of Eq. (1), the force F pushing against the wall of the tube segment is obtained as:

$$F \approx kT\frac{Nb^2}{a^3} \tag{2}$$

Notice the sensitivity of this force to the tube diameter a, which appears as a^3. It is understood that the kinetic pressure of Eq. (1) (or the corresponding force of Eq. (2) is balanced at equilibrium, i.e., when the tube diameter is a_0. Conversely, if flow modifies the tube diameter, a driving force towards equilibrium arises, which we assume to be given by:

$$F \approx kTNb^2\left(\frac{1}{a^3}-\frac{1}{a_0^3}\right) \tag{3}$$

As mentioned above, we assume that tubes tend to be

*Corresponding author: marrucci@unina.it

squeezed affinely by the incoming flow, and since they are essentially aligned to the stretching direction, we may write:

$$\dot{a}_{affine} \approx -\dot{\varepsilon} a \tag{4}$$

where $\dot{\varepsilon}$ is the extension rate of the flow. In our previous work, we derived the steady state situation for any given $\dot{\varepsilon}$, by equating the force of Eq. (3) to the friction force $-\zeta \dot{a}_{affine}$, i.e.:

$$kTNb^2\left(\frac{1}{a^3}-\frac{1}{a_0^3}\right) \approx \zeta \dot{\varepsilon} a \tag{5}$$

Equation (5) predicts that a decreases with increasing $\dot{\varepsilon}$, soon approaching the asymptotic power law $a \propto \dot{\varepsilon}^{-1/4}$.

To calculate the elongational stress in the well aligned case, one should note that, while a decreases, the tube length L correspondingly increases so as to maintain equilibrium in the monomer density along the tube, the equilibrium relationship between a and L being $aL = Nb^2$ (Doi and Edwards, 1986). Assuming monomer density equilibrium along the tube implies that the *longitudinal* friction is ineffective in stretching the chain, i.e., that $\dot{\varepsilon}$ (though large enough to orient and stretch the tubes) remains smaller than the reciprocal Rouse time τ_R of the chain. Under these conditions, the elongational stress σ is given by Marrucci and Ianniruberto (2004).

$$\sigma \approx \nu kT \frac{Nb^2}{a^2} \tag{6}$$

where νN is the number of monomers per unit volume. In view of the scaling law for a, the elongational stress is predicted to scale in proportion with $\dot{\varepsilon}^{1/2}$, in full agreement with Hassager's data (Hassager *et al.*, 2003).

The force balance of Eq. (5) describes a steady state. If, conversely, a transient situation is considered, a new time constant τ_p naturally emerges from the dynamics of the tube diameter. The new time is strictly related to the *lateral* friction coefficient ζ of Eq. (5) in the following way (Marrucci and Ianniruberto, 2004):

$$\tau_p = \frac{\zeta a_0^4}{kTNb^2} \approx \frac{a_0^2}{b^2}\tau_R \tag{7}$$

The last equality in Eq. (7) comes out by arguing on the meaning of the lateral friction coefficient ζ. Such a friction is related to the process where a chain blob fluctuates in size while the surrounding chains relax the corresponding disturbance through a longitudinal retraction within their own tubes. It is through such a mechanism that the Rouse time τ_R of the chains appears in the picture. Eq. (7) thus shows that the relaxation time τ_p of the tube diameter scales with the polymer molecular mass M like a Rouse time, and yet is much larger than τ_R because of the factor a_0^2/b^2. The predicted proportionality between τ_p and M^2 also is in good agreement with Hassager's data.

The model summarized so far is limited to the particular situation of tubes fully oriented in the elongational direction (Marrucci and Ianniruberto, 2004). We here extend the model to arbitrary situations, in which tube segments are variously oriented, and variously deformed. For simplicity, we will assume that the tube cross section is circular at all times, though the tube diameter changes. In other words, the possibility that the tube cross section becomes somewhat elliptical is ignored in the present derivation.

With the latter simplification the model only requires the following state variables of the tube segment: the nondimensional coordinate s along the chain (actually the half-chain $0 < s < \lambda$, where λ is the tube stretch as detailed later, and $\lambda = 1$ at equilibrium), the orientation $\boldsymbol{u}$ ($u^2 = 1$), and the diameter a. Consistently with the classical Doi-Edwards theory, the orientation $\boldsymbol{u}$ is made to change affinely.

$$\dot{\boldsymbol{u}} = \dot{\boldsymbol{u}}_{affine} = (\mathbf{1} - \boldsymbol{uu}) \cdot \boldsymbol{k} \cdot \boldsymbol{u} \tag{8}$$

where $\boldsymbol{k}$ is the velocity gradient of the flow, and $\mathbf{1}$ is the unit tensor. However, $\boldsymbol{u}$ goes back to randomness at the chain end, i.e., at $s = \lambda$ ($s = 1$ at equilibrium). At equilibrium, motion of tube segments along the chain is governed by diffusion only, i.e., by the Langevin equation

$$\dot{s} = f_s \quad \langle f_s \rangle = 0, \quad \langle f_s(t) f_s(t') \rangle = 2D\delta(t-t') \tag{9}$$

where f_s is a random Gaussian term with the moments indicated, D is the chain longitudinal diffusivity, and $\delta(\ldots)$ is the Dirac delta function. Because the chain length has been made nondimensional, D is equivalent to the inverse reptation time τ_d (to within the numerical factor $\pi^2/4$ (Doi and Edwards, 1986)).

Constraint release can be included in the model by adopting, in the numerical simulations, the "trick" of coupling segments in pairs. Hence, whenever one segment of the pair reaches the chain end, the partner segment also gets randomized. During flow, convective constraint release (CCR) also becomes important. Although, for numerical stability, we do not include in Eq. (9) a convective term, CCR is accounted for by calculating the relative velocity between chain end and tube, from which the loss of tube segments by convection can also be reckoned. We then randomize the orientation of an equal number of segments, with their coordinate s randomly chosen.

We now move on to describe the dynamics of the tube diameter a. We write the rate of change of a (made nondimensional by taking the ratio to the most probable equilibrium value a_0) in the following way:

$$\dot{a} = \dot{a}_{affine} + \tau_p^{-1}(a^{-3} - 1) + f_a \tag{10}$$

where the first two terms on the right hand side correspond to those appearing in Eq. (5) when accounting for the definition of τ_p as in Eq. (7). The last term, f_a, is a random Gaussian term, with the following moments

$$\langle f_a \rangle = 0 \; ; \; \langle f_a(t) f_a(t') \rangle = 2\tau_p^{-1}\delta(t-t') \tag{11}$$

where, in view of the non-dimensionality of a, the reciprocal time τ_p^{-1} plays the role of a transversal diffusion coefficient. Because of the stochastic term, the tube diameter a is continuously distributed over a set of values. In view of the force term in Eq. (10), the equilibrium distribution is given by

$$\psi_0(a) = C\exp\left(-\frac{1}{2a^2}-a\right) \tag{12}$$

Equation (12) shows that $a=1$ (i.e., $a=a_0$) is the most probable value, while the average value of a is somewhat larger than unity.

Relaxation of the tube diameter towards equilibrium occurs in two ways. One is through the "lateral" dynamics described by Eqs. (10-11). The second is through the "longitudinal" dynamics due to reptation. Indeed, whenever in the course of the simulation a segment randomizes its orientation $\boldsymbol{u}$ because of reptation, we also randomize its diameter a by picking a new value according to the equilibrium distribution $\psi_0(a)$. Notice that, conversely, when an "internal" tube segment randomizes its orientation because of constraint release, the tube diameter is assumed not to change.

The fact that the tube diameter can go back to equilibrium in two ways, i.e., either in a time τ_p by pushing back the surrounding constraints or in a time τ_d by reptating out, has important consequences. Indeed, depending on the ratio τ_d/τ_p, the transition from the linear behaviour to the asymptotic power law occurs in a qualitatively different way, as discussed in (Marrucci and Ianniruberto, 2004), and later confirmed by experiment (Hassager, 2004).

The dynamics is completed by specifying the average tube stretch λ determined by the change in tube diameter. It is to be made clear that no other chain stretch is here considered, namely the stretch arising when the strain rate becomes larger that the reciprocal Rouse time (because of longitudinal friction) is here ignored. With this assumption, and by recalling the relationship previously mentioned between tube-segment length L and diameter a of the classical Doi-Edwards theory, we take:

$$L \approx Nb^2\langle\frac{1}{a}\rangle \tag{13}$$

There follows:

$$\lambda = \frac{\langle 1/a\rangle}{\langle 1/a\rangle_0} \tag{14}$$

where the denominator in Eq. (14) is the equilibrium average.

In the following section, we will present numerical results obtained with the above described dynamical rules for the case of shear and elongational flows, both at steady state and during start up. Before doing so, however, we must specify the averages that are relevant for the stress tensor. In a previous work (Marrucci and Ianniruberto, 1998) we derived a stress expression that explicitly accounts both for traction along the chain and for pressure exerted on the tube wall. The result there obtained for the general case of elliptical cross section of the tube is readily specified for the simple case of circular cross section as considered here, giving for the nondimensional stress $\boldsymbol{T}$

$$\boldsymbol{T} = \langle\frac{1}{a}\rangle^2\langle\boldsymbol{uu}\rangle + \frac{1}{4}\langle\frac{\boldsymbol{uu}}{a^2}\rangle \tag{15}$$

where the first term arises from chain traction, and the second one from pressure on tube wall.

3. Model predictions

The single nondimensional constitutive parameter of the model is the ratio of relaxation times τ_d/τ_p, which is expected to increase roughly as $M^{1.3\div1.6}$. For the case of polystyrene melts, the analysis reported in (Marrucci and Ianniruberto, 2004) indicates that for $M=200{,}000$ the ratio τ_d/τ_p is nearly unity. We will therefore examine values of that ratio both above and below unity.

Concerning numerical aspects, we used Euler integration in time, and in most cases a population of 30,000 tube segments proved sufficient to obtain good statistics. In slow flows, noise was reduced by using a simple variance reduction technique. In all cases, error bars are within a few percent.

Fig. 1 shows results for steady elongational flows in the form of (nondimensional) tensile stress σ vs. $\dot{\varepsilon}\tau_p$ for several values of τ_d/τ_p, i.e., for various M. These results show the same qualitative features anticipated in Fig. 4 of our

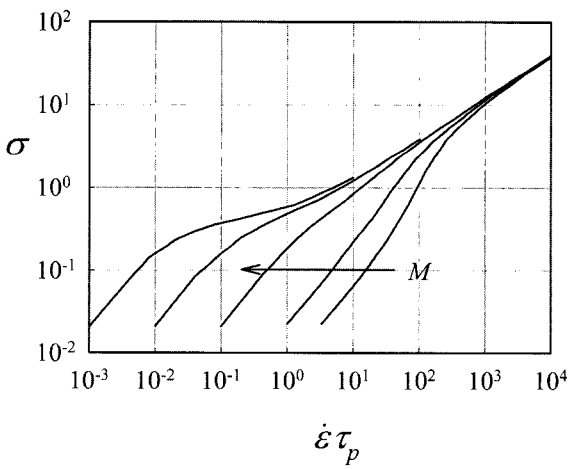

Fig. 1. Nondimensional elongational stress *vs.* $\dot{\varepsilon}\tau_p$ for several values of the time ratio τ_d/τ_p, corresponding to different M. From right to left $\tau_d/\tau_p = 0.03$, 0.1, 1, 10, 100.

previous work (Marrucci and Ianniruberto, 2004), and confirmed by the more recent data of Hassager (2004) (see his Fig. 2). Notice in particular the two rightmost curves in Fig. 1 for low M's, which exhibit an elongational viscosity higher than the Trouton value in the transition from the linear range to the asymptotic power law $\sigma \approx (\dot{\varepsilon}\tau_p)^{1/2}$.

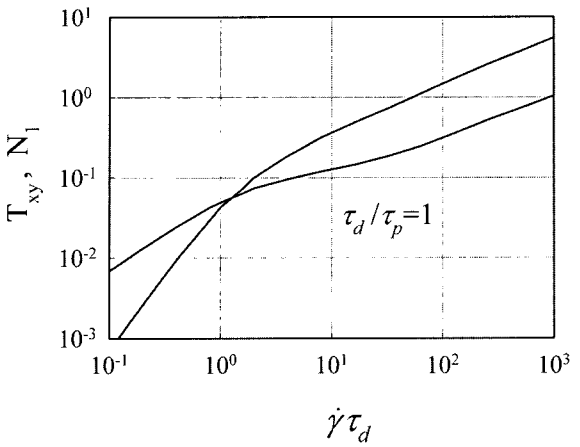

Fig. 2. Shear stress and normal stress difference in steady shear flows for $\tau_d/\tau_p = 1$.

Fig. 2 reports steady shear results for tangential and normal stresses for the case $\tau_d/\tau_p = 1$. Notice that a quasi-plateau for the tangential component is found before yielding towards the asymptotic 1/2 power law. It is noteworthy that such a plateau-like region is found in shear, while (for the same values of τ_d/τ_p) in elongational flow the transition from linear to asymptotic behaviour occurs rather abruptly (middle curve in Fig. 1). This difference between the two flows can be understood by examining what happens to the tube diameter a in the two cases. Fig. 3 indeed shows that the elongational flow is more effective than shear in squeezing the tubes. In its turn, this difference in behaviour is related to the well known fact that elongational flow, differently from shear, is irrotational.

Fig. 4 is the analogous of Fig. 2 for $\tau_d/\tau_p = 10$, i.e., for a larger value of M. The plateau-like region for the shear stress is here more pronounced, and a slight inflection also

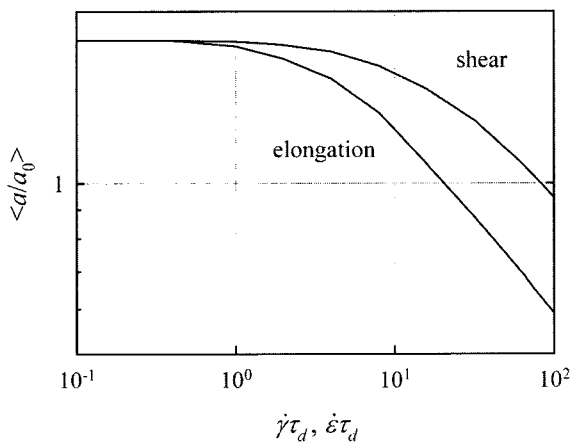

Fig. 3. Average tube diameter in steady shear and elongational flows for $\tau_d/\tau_p = 1$.

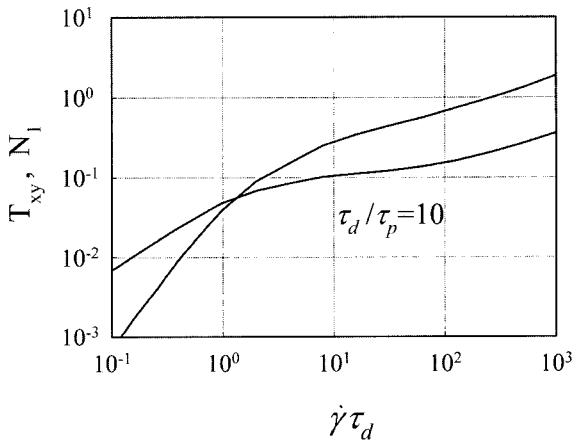

Fig. 4. Same as Fig. 2, but for a larger value of the time ratio τ_d/τ_p, i.e., for higher M.

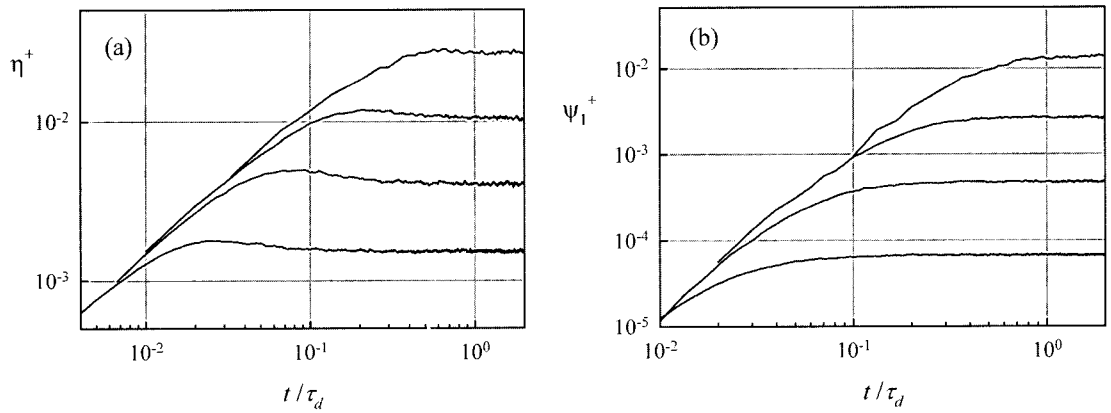

Fig. 5. Curves of transient viscosity (a) and normal stress coefficient (b) in shear start-up for $\tau_d/\tau_p = 10$. Shear rates are $\dot{\gamma}\tau_d = 3$, 10, 30, 100, from top to bottom.

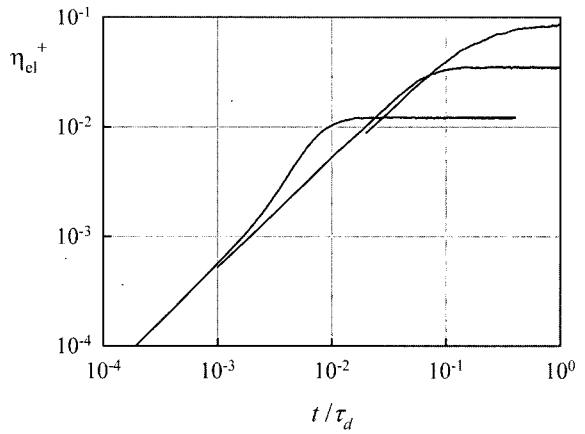

Fig. 6. Curves of transient viscosity in elongational start-up for $\tau_d/\tau_p = 1$. Elongation rates are $\dot{\varepsilon}\tau_d = 10$, 100, 1000, from top to bottom.

appears in the normal stress curve. Altogether, however, the qualitative appearance is not very different at higher *M*. These steady shear results are compatible with recent data by Öttinger *et al.* (2004) on the same melt as used by Hassager in elongation.

Moving now to transient flows, Fig. 5 reports typical results of tangential and normal stresses in start up of shear. The tangential component exhibits overshoots when the shear rate reaches the value $\dot{\gamma}\tau_d \cong 1$, as typically shown by data. As regards the normal component, overshoots in Fig. 5 are suppressed by CCR. This aspect requires further investigation. Finally, Fig. 6 shows the transient viscosity in start up of elongational flows for several values of $\dot{\varepsilon}$. The qualitative features shown in Fig. 6 are in good agreement with Hassager's data (Hassager *et al.*, 2003). Particularly noteworthy is the strain hardening effect. Such a behaviour is predicted (and shown by the data) when the steady elongational viscosity falls in the asymptotic power-law regime of Fig. 1.

4. Conclusions

The model presented in this paper appears promising in describing the nonlinear behaviour of entangled polymer melts, though challenging aspects remain, especially for the case of solutions. In steady uniaxial elongational flows at high stretching rates, the model predicts the power law observed by Hassager *et al.* (2003; 2004) The *M*-dependence of the asymptotic power law is also interpreted by the model (Marrucci and Ianniruberto, 2004). Still in steady elongational flows, the transition from the linear Trouton regime to the asymptotic power law is predicted to show different qualitative features depending on *M* (see Fig. 1). In particular, for moderately entangled melts the model predicts that the elongational viscosity first rises above the Trouton value, and then decreases towards the asymptotic power law. Such an unusual behaviour, anticipated in (Marrucci and Ianniruberto, 2004) and confirmed here, has been experimentally found long ago by Münstedt (1980) as well as very recently by Hassager (2004).

It is to be emphasized, however, that the model presented here appears to represent melts better than solutions. Indeed, yet unpublished data by Sridhar *et al.* (2005) do show a power law behaviour similar to that reported by Hassager *et al.* (2003) but the power comes out significantly different. It so appears that the model presented here needs to be further implemented for possible application to concentrated solutions.

In steady shear flows, the model predicts a plateau-like region of the flow curve, which extends well into the nonlinear region, before yielding to the asymptotic power law. The quasi-plateau is a characteristic feature of the experimental flow curves for monodisperse polymers. Still in steady shear flows, the normal stress difference does not show a plateau, and keeps growing with increasing shear rate with a significant slope. Also this feature is in line with observations. Notice in this regard that CCR theories without chain stretch predict that both tangential and normal stresses approach a plateau. Also predictions of the model in shear and elongational start up mostly exhibit the correct qualitative features, though challenges remain in the magnitude of the overshoots in shear.

As a final note, it is worth mentioning that the results presented here do not differ much from a previous simplified 2D version of the model (Marrucci and Ianniruberto). Even the 3D version presented here, however, requires further development, not only to account for differences between melts and solutions as mentioned above, but also to remove some of the arbitrary assumptions adopted so far for the sake of simplicity.

Acknowledgments

One of the authors (G.I.) acknowledges financial support from the Campania regional government (Regional Bill n°5 dated 28.05.2002).

References

Doi, M. and S.F. Edwards, 1986, The Theory of Polymer Dynamics, Clarendon Press, Oxford.

Hassager, O., A. Bach, K. Almdal and H.K. Rasmussen, 2003, Elongational viscosity of narrow molar mass distribution polystyrene, *Macromolecules* **36**, 5174-5179.

Hassager, O., 2004, Polymer fluid mechanics: molecular orientation and stretching, Proc. XIVth Int. Congr. on Rheology, 22-27 August 2004, Seoul (Korea), NF01-1.

Marrucci, G. and G. Ianniruberto, 1998, Stress tensor and stress-optical law in entangled polymers, *J. Non-Newtonian Fluid Mech.* **79**, 225-234.

Marrucci, G. and G. Ianniruberto, 2004, Interchain pressure effect

in extensional flows of entangled polymers, *Macromolecules* **36**, 3934-3942.

Marrucci G. and G. Ianniruberto, A 2D model for tube orientation and tube squeezing in fast flows of polymer melts, *J. Non-Newtonian Fluid Mech.* **28**, 42-49.

Münstedt, H., 1980, Dependence of the elongational behaviour of polystyrene melts on molecular weight and molecular weight distribution, *J. Rheol.* **24**, 847-867.

Öttinger, H. C., T. Schweizer and J. van Meerveld, 2004, Nonlinear shear rheology of polystyrene melt with narrow molecular weight distribution-Experiment and theory, *J. Rheol.* **48**, 1345-1363.

Sridhar, T., P.K. Bhattacharjee and D.A. Nguyen, 2005, Some unresolved issues of extensional rheology of entangled polymer systems, Wales Conference on Elongational Flow.

Wagner, M.H. and J. Schaeffer, 1992, Nonlinear strain measures for general biaxial extension of polymer melts, *J. Rheol.* **32**, 1-26.

Wagner, M.H., P. Rubio and H. Bastian, 2001, The molecular stress function model for polydisperse polymer melts with dissipative convective constraint release, *J. Rheol.* **45**, 1387-1412.